Biophysical Chemistry 134 (2008) 64–71

Biophysical Chemistry

http://www.elsevier.com/locate/biophyschem

Energetics of OCP1–OCP2 complex formation

Anmin Tan [a], John J. Tanner [a,b], Michael T. Henzl [a,*]

[a] Department of Biochemistry, University of Missouri, Columbia, MO 65211, United States
[b] Department of Chemistry, University of Missouri, Columbia, MO 65211, United States

Received 28 December 2007; received in revised form 17 January 2008; accepted 17 January 2008
Available online 1 February 2008

Abstract

OCP1 and OCP2, the most abundant proteins in the cochlea, are putative subunits of an SCF E3 ubiquitin ligase. Previous work has demonstrated that they form a heterodimeric complex. The thermodynamic details of that interaction are herein examined by isothermal titration calorimetry. At 25 °C, addition of OCP1 to OCP2 yields an apparent association constant of 4.0×10^7 M^{-1}. Enthalpically-driven ($\Delta H=-35.9$ kcal/mol) and entropically unfavorable ($-T\Delta S=25.5$ kcal/mol), the reaction is evidently unaccompanied by protonation/deprotonation events. ΔH is strongly dependent on temperature, with $\Delta C_p=-1.31$ kcal mol^{-1} K^{-1}. Addition of OCP2 to OCP1 produces a slightly less favorable ΔH, presumably due to the requirement for dissociation of the OCP2 homodimer prior to OCP1 binding. The thermodynamic signature for OCP1/OCP2 complex formation is inconsistent with a rigid-body association and suggests that the reaction is accompanied by a substantial degree of folding.

Keywords: Ubiquitin ligase; SCF complex; F-box protein; Organ of Corti; Cochlea; ITC

1. Introduction

The organ of Corti (OC), the mammalian auditory organ, contains sensory and non-sensory cells. The sensory cell population includes the *inner*- and *outer hair cells*, responsible for acoustic signal transduction and amplification, respectively. The non-sensory cell population, also known as the supporting cell population or epithelial support complex (ESC), includes 12 morphologically distinct cell types [1]. The ESC sub-populations share two characteristics — an extensive gap-junction network and high-level expression of OCP1 and OCP2.

OCP1 and OCP2 comprise approximately 10% of the total cell protein in the OC [2]. Although their physiological role is presently unknown, sequence analysis suggests that they are components of an SCF E3 ubiquitin ligase. SCF complexes direct ubiquitination of specific target proteins. Ubiquitination is widely regarded as the signal for destruction by the 26S proteasome [3]. However, ubiquitin is known to have additional signaling functions. Recognition by the proteasome requires polyubiquitination ($N\geq4$). Mono-, di-, and tri-ubiquitinated species are not degraded. Protein translation, activation of protein kinases and transcription factors, and DNA repair are examples of ubiquitin-dependent phenomena not involving proteolysis [4].

Since their discovery in yeast [5,6], SCF ligases have been found in all eukaryotic species [7]. SCF is an acronym for *S*kp1, *c*ullin, and *F*-box protein. Cullin – named for the Cul1 gene product in yeast – serves as the scaffold for complex assembly [8–10]. Skp1 and the ubiquitin-conjugating enzyme (the E2 ligase) bind to cullin. The F-box protein, which dictates target protein specificity [11], binds to Skp1 through a characteristic F-box motif, present in the N-terminal half of the sequence. Interactions with the C-terminal domain of the F-box protein evidently position the target protein for ubiquitination by the E2 conjugating enzyme. The protein known as Rbx1 or Roc1 is also a subunit of the SCF complex [12].

The 163-residue sequence of OCP2 is identical to that of Skp1, although OCP2 is reportedly transcribed from a distinct

* Corresponding author. Department of Biochemistry, 117 Schweitzer Hall, University of Missouri, Columbia, MO 65211, United States. Tel.: +1 573 882 7485; fax: +1 573 884 4812.
E-mail address: henzlm@missouri.edu (M.T. Henzl).

0301-4622/$ - see front matter © 2008 Elsevier B.V. All rights reserved.
doi:10.1016/j.bpc.2008.01.005

gene [13]. The 299-residue sequence of OCP1 [14] harbors an F-box motif and exhibits 81% identity to Fbs1, or neural F-box protein [15]. OCP1 and OCP2 form a high-affinity heterodimeric complex [16]. Although several Skp1/F-box protein complexes have been characterized structurally, there is a paucity of thermodynamic data for the interaction. In this paper, we examine the energetics of OCP1–OCP2 complex formation by isothermal titration calorimetry (ITC).

2. Experimental

2.1. Reagents and chemicals

NaCl, $CaCl_2 \cdot H_2O$, $MgCl_2 \cdot 2H_2O$, trishydroxymethylaminomethane (Tris), monobasic anhydrous sodium phosphate (NaP_i), 4-(2-hydroxyethyl)-1-piperazineethanesulfonic acid (Hepes), lysozyme, and Spectrapor 2 dialysis tubing (MWCO 12,000–14,000) were purchased from Fisher Scientific Co. Luria-Bertani (LB) broth (Miller), LB agar (Miller), ampicillin, kanamycin, and chloramphenicol were obtained from Research Products International. Isopropylthio-β-D-galactoside (IPTG) and dithiothreitol (DTT) were purchased from Gold Biotechnology. Diethylaminoethyl-Sepharose (DEAE-Sepharose), Sephadex G-75, Sephacryl S-100 HR, and trishydroxypropyl phosphine (THP) were obtained from Sigma-Aldrich Co. Complete® protease inhibitor tablets were obtained from Roche Applied Science. $^{15}NH_4Cl$ was purchased from Cambridge Isotope Laboratories.

2.2. Protein expression and purification

2.2.1. OCP2

The OCP2 coding sequence was cloned into pTriEx-1.1 (Novagen), between the NcoI and BamHI sites. That construction was used to transform *E. coli* BL21(DE3) Rosetta 2 cells (Novagen). Bacteria harboring the OCP2-pTRIex1.1 plasmid were cultured at 37 °C in LB broth containing ampicillin (100 μg/mL) and choramphenicol (30 μg/mL). When the turbidity of the culture, measured at 600 nm, reached 0.6, expression was induced with IPTG (0.25 mM). After an additional 3 h, the bacteria were harvested by centrifugation. The cell paste was resuspended in 20 mM Hepes, pH 7.4, containing protease inhibitors, and lysed by treatment with lysozyme and extrusion from a French pressure cell. The resulting suspension was heat-treated for 5 min at 60 °C, then centrifuged at 4 °C for 30 min at 27,000 ×g. OCP2 was isolated from the clarified lysate by NaCl-gradient (0–0.6 M, in 20 mM Hepes, pH 7.4) elution from DEAE-Sepharose, followed by gel-filtration through Sephadex G-75 in PBS (0.15 M NaCl, 0.010 M NaP_i, pH 7.4) containing 0.001 M DTT. A 1-L culture yields 20–30 mg with purity exceeding 95%.

The identical protocol was used to isolate ^{15}N-labeled OCP2, except that the bacteria were cultured on minimal medium (M9 salts plus glucose) containing 1.25 g $^{15}NH_4Cl$ per liter.

2.2.2. OCP1

The OCP1 coding sequence was cloned into pET28a (Novagen), between the Nde I and BamH I sites, downstream from the hexa-histidine tag and thrombin-cleavage site. Expression – in Rosetta 2 cells, in LB broth containing kanamycin (50 μg/mL) and chloramphenicol – and lysis were performed as described above. OCP1 was isolated from the clarified lysate by binding/elution from Ni-NTA His-Bind resin (Novagen). After overnight dialysis at 4 °C against PBS, the protein was treated, for 4 h on ice, with thrombin (Novagen, 1 U/mg protein). After confirming cleavage, the thrombin was inactivated with PMSF (1 mM) and DTT (10 mM). The preparation was then subjected to gel-filtration through Sephacryl S-100 HR, in PBS and 1 mM DTT. A 1-L culture yields 6–8 mg of OCP1 with purity exceeding 95%.

2.3. Quantitation

OCP1 and OCP2 concentrations were estimated spectrophotometrically. Extinction coefficients at 280 nm – 81,000 and 19,400 M^{-1} cm^{-1}, respectively – were obtained by parallel absorbance and interference measurements in a Beckman XL-I analytical ultracentrifuge.

2.4. Isothermal titration calorimetry

ITC was performed in a MicroCal VP-ITC. Prior to analysis, OCP1 and OCP2 were dialyzed extensively against a common buffer. THP (2.0 mM) was included in the buffer reservoir to maintain the cysteine sulfhydryl groups in the reduced state. Aliquots of the dialysis buffer were used to make dilutions.

Raw ITC data were integrated using the software supplied with the instrument. Single datasets were analyzed using the single-site model. An Origin script was written to simultaneously fit multiple datasets. All titrations included a 2.0 μL pre-injection. The heat associated with that addition, invariably low due to diffusion of titrant from the buret during thermal equilibration, was neglected during the fitting process. The integrated signals from the final three additions in each experiment were averaged and used to estimate the combined heat of mixing/dilution, which was subtracted from the data prior to least-squares minimization.

2.5. NMR spectroscopy

The ^1H,^{15}N-HSQC spectrum of OCP2 was obtained at 30 °C on a Varian Inova 600 MHz spectrometer, employing a triple-resonance cryoprobe equipped with pulsed-field *z* gradient. The 2.0 mM sample contained 0.15 M NaCl, 0.01 M NaP_i, pH 6.0, 0.002 M THP, 5% D_2O. Data were acquired with the BioPack N15-HSQC pulse sequence, processed with NMRPipe [17], and visualized with Sparky [18]. ^1H chemical shifts were referenced relative to sodium 2,2-dimethyl-2-silapentane-5-sulfonate (DSS); the ^{15}N shifts were referenced indirectly.

2.6. Accessible surface area calculations

The surface area buried in the Skp1/Fsb1 interface was analyzed with CNS [19]. Hydrogen atoms were added to the coordinates of the Skp1–Fsb1 complex (PDB code 2E31) using the ALLHDG topology and parameter files. Water molecules

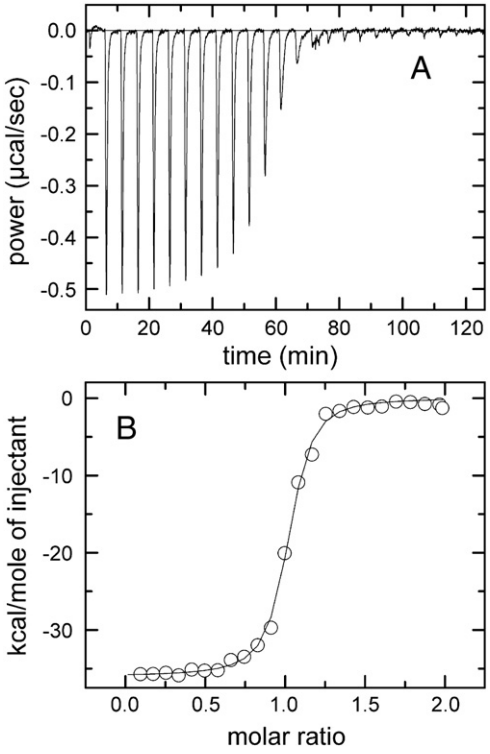

Fig. 1. Titration of OCP2 with OCP1. A sample of 5.0 µM OCP2 was titrated with 50 µM OCP1 at 25 °C in 0.15 M NaCl, 0.025 M Hepes, 0.002 M THP, pH 7.4. (A) Raw differential power data for the reaction. (B) Integrated injection heats plotted against the molar ratio of OCP1 to OCP2.

were omitted. The interfacial area was calculated as the difference in the solvent-accessible surface areas of the isolated proteins and the complex, employing a 1.4 Å probe. For estimation of the polar and apolar contributions to the interface, carbon and sulfur atoms, and hydrogen atoms bonded to C or S, were considered apolar. All other atoms were considered polar.

3. Results

Complex formation between OCP1 and OCP2 was first demonstrated by electrophoretic mobility shift assay (EMSA). Addition of OCP2 to OCP1 yields a new species with reduced electrophoretic mobility. When examined as a function of increasing OCP2 concentration, the mobility shift was shown to be complete at a 1:1 molar ratio of OCP2:OCP1 [16]. If an equimolar mixture of the two proteins is subjected to sedimentation equilibrium, the resulting data can be satisfactorily modeled with the assumption of a single species with M_r 51,000 [16]. This value agrees well with the combined sequence-derived molecular weights of OCP1 and OCP2 (52,300), strongly suggesting that the OCP1/OCP2 complex is a heterodimer.

OCP1/OCP2 complex formation is amenable to study by isothermal titration calorimetry (ITC). Fig. 1A presents representative raw data from a titration of OCP2 (5 µM) with OCP1, at 25 °C in 0.15 M NaCl, 0.025 M Hepes, pH 7.4. It might be noted that these data were collected at 240 s intervals. Increasing the injection interval to 500 s had no perceptible impact on the results, indicating that the analysis was not complicated by slow association kinetics. Fig. 1B displays the enthalpy change for the reaction as a function of the molar ratio of OCP1 to OCP2. The solid line through the points represents the optimal least-squares fit to the data.

OCP1/OCP2 complex formation is highly exothermic, with an apparent $\Delta H°$ equal to −35.9 kcal/mol. The association constant for the reaction, 4.0×10^7 M^{-1}, corresponds to a $\Delta G°'$ of −10.4 kcal/mol. The reaction is highly unfavorable entropically ($-T\Delta S°'=25.5$ kcal/mol). Although qualitatively similar behavior is observed when OCP1 is titrated with OCP2, the accompanying enthalpy change is 1–2 kcal/mol less favorable (Table 1).

If protonation/deprotonation events accompany the binding reaction, then the observed enthalpy will be dependent on the buffer ionization enthalpy according to this equation:

$$\Delta H_{obs} = \Delta H_{bind} + n\Delta H_{buffer} \quad (1)$$

In this equation, ΔH_{bind} represents the intrinsic enthalpy of association, n is the number of protons released, and ΔH_{buffer} represents the buffer ionization enthalpy. To determine whether OCP1/OCP2 complex formation is accompanied by protonation/deprotonation phenomena, the reaction was examined in three

Table 1
Summary of ITC data for OCP1/OCP2 complex formation[a]

Temp	Titrant	buffer	K ($\times10^{-7}$)	ΔG[b]	ΔH	$-T\Delta S$[c]	ΔS
25	OCP1	PBS	4.0 (0.4)	−10.4 (0.1)	−35.9 (0.3)	25.5 (0.4)	−85.6 (1.3)
25	OCP 2	PBS	3.9 (0.4)	−10.4 (0.1)	−34.4 (0.3)	24.0 (0.4)	−80.6 (1.3)
25	OCP 2	Hepes	3. 9 (0.4)	−10.4 (0.1)	−34.1 (0.2)	23.7 (0.3)	−79.6 (1.0)
25	OCP 2	Tris	3.6 (0.4)	−10.3 (0.1)	−34.0 (0.3)	23.7 (0.4)	−79.4 (1.3)
28	OCP 1	PBS	2.8 (0.3)	−10.3 (0.1)	−39.7 (0.2)	29.4 (0.3)	−97.7 (1.0)
28	OCP 2	PBS	2.7 (0.2)	−10.2 (0.1)	−38.1 (0.2)	27.9 (0.3)	−92.5 (1.0)
31	OCP 1	PBS	1.7 (0.1)	−10.1 (0.1)	−43.8 (0.3)	33.7 (0.4)	−111 (1.3)
31	OCP 2	PBS	1.7 (0.2)	−10.1 (0.1)	−42.1 (0.2)	32.0 (0.3)	−105 (1.0)
34	OCP 1	PBS	1.6 (0.2)	−10.1 (0.1)	−47.2 (0.2)	37.1 (0.3)	−121 (1.0)
34	OCP 2	PBS	1.5 (0.1)	−10.1 (0.1)	−45.9 (0.2)	35.8 (0.3)	−117 (1.0)
37	OCP 1	PBS	1.4 (0.2)	−10.1 (0.1)	−51.7 (0.3)	41.6 (0.4)	−134 (1.3)
37	OCP 2	PBS	1.4 (0.1)	−10.1 (0.1)	−50.2 (0.4)	40.1 (0.5)	−129 (1.6)

[a] All reactions conducted at pH 7.4. Temperature is expressed in °C; K is expressed in units of M^{-1}; ΔG, ΔH, and $-T\Delta S$ are expressed in kcal/mol; and ΔS is expressed in units of cal mol^{-1} K^{-1}. Uncertainties are listed in parentheses.

[b] $\Delta G=-RT\ln K$.

[c] $-T\Delta S=\Delta G-\Delta H$.

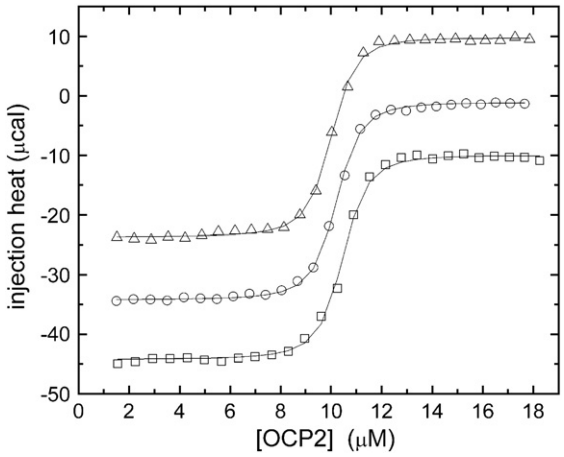

Fig. 2. Titration of OCP1 with OCP2 in buffers of differing ionization enthalpy. 10 μM samples of OCP1 were titrated with 100 μM OCP2, at pH 7.4 and 25 °C, in 0.15 M NaCl, buffered either with 25 mM Hepes (squares), 10 mM phosphate (circles), or 25 mM Tris (triangles). The datasets have been offset vertically for clarity.

buffers having disparate ionization enthalpies — phosphate, Hepes, and Tris. Their respective ionization enthalpies are 1.2 kcal/mol, 5.0 kcal/mol, and 11.3 kcal/mol [20,21].

In these experiments, OCP1 (10 μm) was titrated with OCP2 at 25 °C. Fig. 2 displays the integrated data from all three titrations. The solid line represents the optimum global fit, obtained with the assumption of a common $\Delta H°$ value. The observation that all three experiments can be satisfactorily accommodated by the same apparent reaction enthalpy, −34 kcal/mol, indicates that protonation effects are negligible.

The enthalpy change associated with the OCP1–OCP2 interaction is strongly temperature-dependent. The dependence of ΔH on temperature is given by the relationship:

$$\Delta H(T) = \Delta H(T_r) + \Delta C_p(T - T_r) \quad (2)$$

where $\Delta H(T)$ is the enthalpy change at temperature T, $\Delta H(T_r)$ is the enthalpy change at a reference temperature T_r, and ΔC_p is

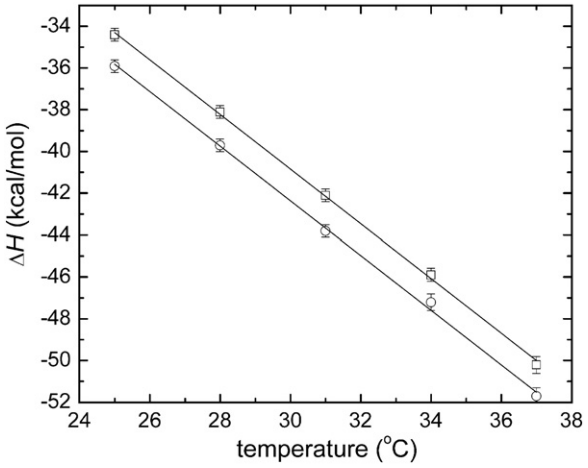

Fig. 3. Temperature-dependence of the OCP1–OCP2 interaction. The interaction between OCP1 and OCP2 was examined, in PBS, as a function of temperature between 25 and 37 °C. Two series of experiments were conducted. In one case, 5.0 μM OCP1 was titrated with 50 μM OCP2 (squares); in the other, 5.0 μM OCP2 was titrated with 50 μM OCP1 (circles).

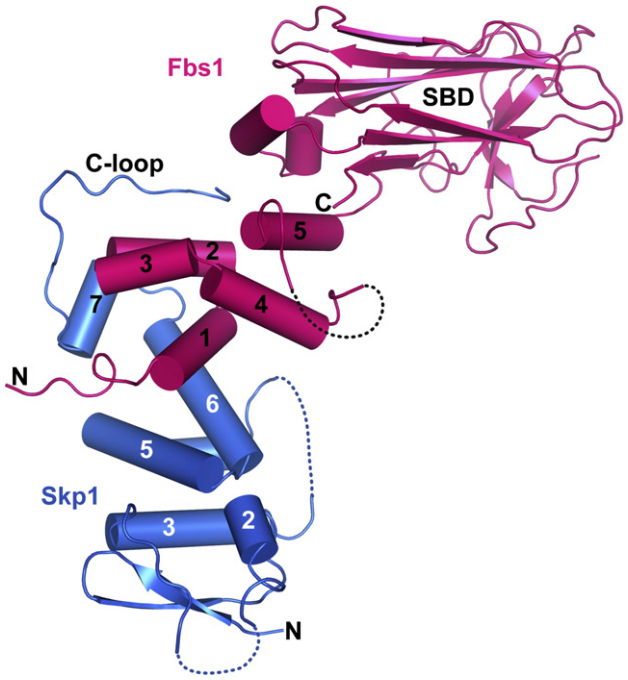

Fig. 4. Diagram of the Skp1/Fbs1 complex. The interface between Skp1 (cyan) and the F-box protein Fbs1 (magenta) is formed by juxtaposition of helices 5–7 and the C-terminal loop of Skp1 with helices 1–4 of Fbs1. Coordinates are from PDB 2E31 [22]. The figure was produced with PyMOL [45]. (For interpretation of the references to color in this figure legend, the reader is referred to the web version of this article.)

the change in the heat capacity resulting from the reaction. Thus, when the enthalpy change associated with a reaction is plotted versus temperature, the slope of the best-fit line through the points provides an estimate for ΔC_p. Over a suitably narrow temperature range, ΔC_p can be treated as a constant.

Fig. 3 displays the enthalpy change of OCP1/OCP2 complex formation as a function of temperature. Two sets of experiments were performed. In one case (○), samples of OCP2 were titrated with OCP1 at 25, 28, 31, 34, and 37 °C. In the other (□), samples of OCP1 were titrated with OCP2 at the same five temperatures. The two datasets yield identical estimates for ΔC_p of -1.31 ± 0.02 kcal mol^{-1} K^{-1}. Although the choice of titrant has no impact on the slope, the two lines are offset vertically by 1.6 kcal/mol.

4. Discussion

OCP1 and OCP2 were discovered during an electrophoretic survey of OC proteins. The two most abundant proteins in the auditory organ, they account for 10% of the total protein. Their distribution coincides with the boundaries of a gap-junction system that unites the non-sensory cells in the OC, fueling speculation that they function in the regulation of gap-junction activity.

Amino acid sequence data suggest that OCP1 and OCP2 are subunits of an SCF E3 ubiquitin ligase:OCP2 is an ortholog of Skp1; and OCP1 harbors an F-box motif and is homologous to the F-box protein known as Fbs1 or NFBP. The latter evidently targets glycoproteins and is believed to mediate the degradation

of misfolded proteins recovered from the endoplasmic reticulum [22].

To the best of our knowledge, the OCP1 and OCP2 expression levels are unrivaled by any other Skp1/F-box protein complex. Moreover, the OC does not appear to contain comparable levels of cullin 1, the scaffold protein in SCF complexes [23]. Therefore, it is possible, if not likely, that the OCP1/OCP2 complex has a function beyond its putative role in an SCF ligase. Thus, the investigation of the OCP1–OCP2 interaction, in the absence of the other SCF subunits, has potential physiological relevance.

Although the structure of the OCP1/OCP2 complex has not been determined, high-resolution structural data are available for several other Skp1/F-box protein complexes. These include Skp1/Skp2 [24] and Skp1/Fbs1 [25]. A cartoon of the latter is displayed in Fig. 4. The F-box domain in Fbs1, which exhibits 90% identity to OCP1, spans residues 55–95 and includes α helices 1–4. The interface between the Skp1 and Fbs1 buries 960 Å^2 and 2520 Å^2 of polar and apolar surface area, respectively. Approximately two-thirds of this interface is produced by contact between F-box helices 1–4 and Skp1 helices 5–7. The remainder results from contact between the C-terminal loop of Skp1 and the opposite face of F-box helices 2 and 3.

The half-life of the Skp1/Skp2 complex reportedly exceeds 9 h ($k_{off}<2\times10^{-5}$ s^{-1}) [24]. Assuming that $k_{on}\geq5\times10^{4}$ M^{-1} s^{-1} for the interaction, a decidedly conservative lower limit, the thermodynamic association constant for the Skp1/Skp2 complex (equal to k_{on}/k_{off}) must exceed 2.5×10^{9} M^{-1}. The OCP1–OCP2 interaction, exhibiting an apparent binding constant at 25 °C of 4.0×10^{7} M^{-1}, is evidently substantially weaker. Slow association kinetics can lead to underestimation of the binding affinity, if insufficient time for equilibration is allowed between injections. However, the raw ITC data for the OCP1–OCP2 interaction show no evidence of kinetic limitation. Following an injection, the differential power trace exhibits a rapid rise time and return to baseline, and the injection heats are independent of the injection interval beyond 240 s. Thus, the relatively low affinity measured for the OCP1/OCP2 complex is not a reflection of slow association. Although the documented self-association behavior of OCP1 and OCP2 [16,26] could reduce the apparent binding affinity, the impact is expected to be relatively minor, as discussed below. It is more likely that the observed difference in affinity has a structural basis.

Although the interactions between Skp1 and the F-box motif are similar in the Skp1/Skp2 and Skp1/Fbs1 complexes, they are not identical. Notably, whereas the C-terminal peptide of Skp1 adopts a helical conformation in the Skp1/Skp2 complex, it adopts a loop structure in the Skp1/Fbs1 complex. The helix is presumably destabilized by the encroachment of helix 2 from Fbs1. Because the OCP1–OCP2 interaction surface is expected to resemble that in Skp1/Fbs1, an unfavorable steric interaction between helix 2 in OCP1 and the C-terminal sequence of OCP2 could contribute to the reduced stability of the OCP1/OCP2 complex, relative to Skp1/Skp2.

The apparent binding constant at 25 °C corresponds to a $\Delta G^{\circ\prime}$ value of −10.4 kcal/mol. The reaction is driven by a large enthalpy change, −35.9 kcal/mol, and is entropically unfavorable, with a $-T\Delta S^{\circ\prime}$ term of 25.4 kcal/mol. The enthalpy of complex formation is independent of the buffer ionization enthalpy, indicating that protonation phenomena do not contribute significantly to the observed enthalpy change.

Interestingly, the magnitude of the enthalpy change for the reaction is perceptibly smaller when OCP2 is the titrant. This phenomenon presumably reflects the strong self-associative tendency of OCP2 [26]. With a K_d in the low μM range, OCP2 will be substantially monomeric when titrated with OCP1, due to the relatively low concentration (5–10 μM) of the protein in the sample cell. By contrast, it will be largely dimeric at the concentrations present in the buret (50–100 μM). Thus, when OCP2 is the titrant, the observed ΔH will include a larger contribution from the enthalpy of OCP2 dissociation. Although we do not presently have a precise estimate for this quantity, preliminary sedimentation data (not shown) indicate that dissociation is endothermic, consistent with the observed reduction in exothermicity. In this context, it should be noted that OCP1 also dimerizes [16]. However, that interaction is substantially weaker.

What impact will self-association of OCP1 and OCP2 have on the apparent free energy change for heterodimer formation? Allowing for the self-associative tendencies of OCP1 and OCP2, we can write the following equilibria:

$$2\mathrm{OCP1}\overset{K_{11}}{\rightleftharpoons}(\mathrm{OCP1})_2;K_{11}=\frac{\left[(\mathrm{OCP1})_2\right]}{[\mathrm{OCP1}]^2} \tag{3}$$

$$2\mathrm{OCP2}\overset{K_{22}}{\rightleftharpoons}(\mathrm{OCP2})_2;K_{22}=\frac{\left[(\mathrm{OCP2})_2\right]}{[\mathrm{OCP2}]^2} \tag{4}$$

$$\mathrm{OCP1}+\mathrm{OCP2}\overset{K_{12}}{\rightleftharpoons}\mathrm{OCP1}\bullet\mathrm{OCP2};K_{12}=\frac{[\mathrm{OCP1}\bullet\mathrm{OCP2}]}{[\mathrm{OCP1}][\mathrm{OCP2}]} \tag{5}$$

K_{11} and K_{22} – the equilibrium constants for homodimer formation by OCP1 and OCP2 – are on the order of 10^5 M^{-1} and 10^6 M^{-1}, respectively [16,26]. In Eq. (5), K_{12} represents the true heterodimer association constant. The observed, or apparent, association constant K_{12}' is related to K_{12} by the relationship:

$$\begin{aligned}K_{12}^{'}&=\frac{[\mathrm{OCP1}\bullet\mathrm{OCP2}]}{\left([\mathrm{OCP1}]+2\left[(\mathrm{OCP1})_2\right]\right)\left([\mathrm{OCP2}]+2\left[(\mathrm{OCP2})_2\right]\right)}\\&=K_{12}\frac{1}{(1+2K_{11}[\mathrm{OCP1}])(1+2K_{22}[\mathrm{OCP2}])}\end{aligned} \tag{6}$$

so that

$$K_{12}=K_{12}^{'}(1+2K_{11}[\mathrm{OCP1}])(1+2K_{22}[\mathrm{OCP2}]). \tag{7}$$

For illustration, assume that 1.4 mL of 1×10^{-5} M OCP2 is titrated with 0.01 mL aliquots of 1.0×10^{-4} M OCP1. Eqs. (3)–(6) can be solved to obtain the (free) concentrations of OCP1 and OCP2 at the mid-point in the titration, 1.42×10^{-7} M and 1.37×10^{-6} M, respectively. Substituting these values into Eq. (7) yields $K_{12}=1.5\times10^{8}$ M^{-1}. Thus, the observed heterodimer association constant (4×10^{7} M^{-1}) is roughly 3.8 times smaller than the true value, corresponding to an error, at 298 K, of approximately 0.8 kcal/mol.

Proteins exhibit a broad spectrum of flexibility. Many protein–protein associations approximate rigid-body interactions, accompanied by modest conformational changes. The binding of turkey ovomucoid third domain to elastase is a particularly well-studied example [27]. In stark contrast, the folding event that accompanies association of HIV envelope glycoprotein (GP120) and CD4 involves nearly one hundred residues [28]. In the following paragraphs, we show that the behavior of the OCP1–OCP2 reaction is more reminiscent of the latter system.

If OCP1/OCP2 complex formation were unaccompanied by a significant conformational alteration, then the observed ΔH and ΔC_p values would be largely attributable to the changes in polar and apolar surface area. Employing the scaling factors reported by Xie and Freire [29], the enthalpy change at 60 °C, $\Delta H(60)$, and the change in heat capacity for a process can be related to the associated changes in surface area through these equations:

$$\Delta H(60) = 31.4\Delta\mathrm{ASA}_p - 8.44\Delta\mathrm{ASA}_{ap} \quad (8)$$

$$\Delta C_p = 0.45\Delta\mathrm{ASA}_{ap} - 0.26\Delta\mathrm{ASA}_p \quad (9)$$

where $\Delta H(60)$ and ΔC_p are expressed in units of cal mol^{-1} and cal mol^{-1} K^{-1}, respectively, and $\Delta\mathrm{ASA}_p$ and $\Delta\mathrm{ASA}_{ap}$ represent the changes in solvent-accessible polar and apolar surface area, respectively, in Å^2.

Given the sequence similarity between OCP1 and Fbs1 (90% identity in the F-box motif), the interface between OCP1 and OCP2 is expected to resemble the Skp1/Fbs1 interface — with $\Delta\mathrm{ASA}_p$ and $\Delta\mathrm{ASA}_{ap}$ values of −960 and −2520 Å^2, respectively. Substitution of these values into Eqs. (8) and (9) affords estimates for ΔC_p and $\Delta H(60)$ of −0.88 kcal mol^{-1} K^{-1} and −8.88 kcal/mol. Extrapolation of $\Delta H(60)$ yields a predicted enthalpy change at 25 °C of +22.1 kcal/mol. The disparity between the calculated and observed values of ΔC_p and $\Delta H(25)$ (−1.31 kcal mol^{-1} K^{-1} and −35.9 kcal/mol, respectively) strongly suggests that the observed thermodynamics are inconsistent with a rigid-body interaction.

The correlation between ΔC_p and accessible surface area derived by Xie and Freire [29] incorporated cyclic peptide dissolution data [30], as well as protein denaturation data. Robertson and Murphy obtained somewhat different fitting coefficients based exclusively on thermal denaturation data for a set of 49 proteins [31]:

$$\Delta H(60) = 20.54\Delta\mathrm{ASA}_p - 1.91\Delta\mathrm{ASA}_{ap} \quad (10)$$

$$\Delta C_p = 0.16\Delta\mathrm{ASA}_{ap} + 0.12\Delta\mathrm{ASA}_p \quad (11)$$

Using the aforementioned $\Delta\mathrm{ASA}_p$ and $\Delta\mathrm{ASA}_{ap}$ values, these parameters return values for ΔC_p and $\Delta H(60)$ of −0.52 kcal mol^{-1} K^{-1} and −14.9 kcal/mol. Extrapolating the enthalpy change to 25 °C yields a value of +3.3 kcal/mol. Clearly, the conclusion that the energetic signature of the OCP1–OCP2 association is incompatible with a rigid-body association is independent of the structural parametrization scheme employed.

The ΔASA values derived from analysis of the Skp1/Fbs1 structure assume reaction between Skp1 and Fbs1 monomers. Because OCP2 and OCP1 are capable of forming homodimers, as noted above, the actual net change in accessible surface area upon heterodimer formation could be smaller. This circumstance would impact the calculated values for ΔC_p and $\Delta H(60)$, but would not alter the fundamental conclusion. For example, a 50% reduction in the magnitudes of $\Delta\mathrm{ASA}_p$ and $\Delta\mathrm{ASA}_{ap}$ yields a ΔC_p of −0.44 kcal mol^{-1} K^{-1} and $\Delta H(60)$ of −4.5 kcal/mol, employing the Xie and Freire correlations in Eqs. (8) and (9).

As noted above, OCP1–OCP2 complex formation is entropically unfavorable. At 25 °C, the overall entropy change for the protein–protein association, ΔS_{assoc}, is −86 cal mol^{-1} K^{-1}. This quantity reflects the sum of several terms:

$$\Delta S_{assoc} = \Delta S_{solv} + \Delta S_{rt} + \Delta S_{conf} \quad (12)$$

ΔS_{solv} is the entropy contribution due to changes in solvation; ΔS_{rt} represents the entropy contribution resulting from restricted rotational and translational motion; and ΔS_{conf} is the entropy component resulting from changes in conformation, including folding.

The entropy of solvation, polar and apolar, approaches zero at 385 K [32,33]. Thus, the solvation entropy change at 25 °C can be estimated from the relationship:

$$\Delta S_{solv} = \Delta C_p \ln\left(\frac{298.15}{385.15}\right) \quad (13)$$

When substituted into this equation, the observed ΔC_p value of −1310 cal mol K^{-1} yields a solvation entropy contribution of 335 cal mol^{-1} K^{-1}.

The ΔS_{rt} term has been the subject of controversy. Statistical thermodynamic calculations [34,35] have suggested that protein–protein association should reduce the rotational and translational entropies of the system by roughly 50 cal mol^{-1} K^{-1} apiece. Values between −50 and −100 e.u. have been widely applied in the analysis of protein–protein and protein–nucleic acid complexes [36–38]. On the other hand, Amzel [39] has argued that the loss of translational entropy should not exceed −10 cal mol^{-1} K^{-1}. Moreover, an elegant DSC comparison of monomeric and disulfide-linked dimeric forms of a subtilisin

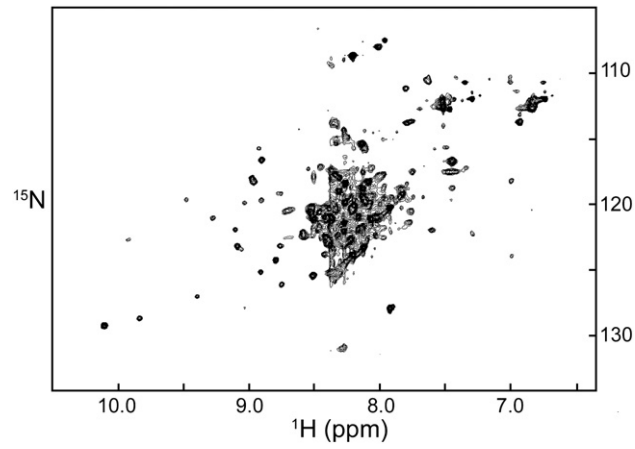

Fig. 5. ^{1}H,^{15}N-HSQC spectrum of OCP2. Data were collected at pH 6.0 and 30 °C. Note the cluster of intense peaks centered around 8.3 ppm in the proton dimension.

inhibitor yielded an estimate for the translational entropy decrease of −5±4 cal mol^{-1} K^{-1} [40]. Baker and Murphy [27] contend that the rotational and translational entropy contributions are effectively accounted for by the classical "cratic" entropy term, a statistical correction for the mixing of solute and solvent molecules:

$$\Delta S_{\mathrm{mix}} = R\ln\left(\frac{1}{55.5}\right) = 8.0\,\mathrm{cal\ mol^{-1}K^{-1}} \quad (14)$$

This approximation will be employed in the present calculation.

Rearranging Eq. (12) and solving for ΔS_{conf} yields:

$$\Delta S_{\mathrm{conf}} = \Delta S_{\mathrm{assoc}} - \Delta S_{\mathrm{solv}} - \Delta S_{\mathrm{rt}} \quad (15)$$

Substituting the observed $\Delta S_{\mathrm{assoc}}$ value (−86 e.u.) and the calculated ΔS_{solv} value (335 e.u.) into Eq. (8), and replacing ΔS_{rt} with $-\Delta S_{\mathrm{mix}}$, we obtain an estimate for ΔS_{conf} of −413 cal mol^{-1} K^{-1}. This value is comparable in magnitude to the conformational entropy change associated with the folding of small proteins.

Formation of the OCP1/OCP2 complex is apparently accompanied by the ordering of numerous residues on one, or both, proteins. Spolar and Record [38] have suggested that the number of residues participating in a linked folding transition, N_{fold}, can be estimated by dividing ΔS_{conf} by −5.6:

$$N_{\mathrm{fold}} = \frac{\Delta S_{\mathrm{conf}}}{-5.6} \quad (16)$$

For the present case, this formula indicates that 74 residues are involved.

Robertson and Murphy [31] also derived correlations between changes in ΔC_p and $\Delta H(60)$ and the change in number of solvent-accessible residues accompanying a transition. Their heat capacity-based scaling factor is 13.9 cal K^{-1} (mol res)$^{-1}$. Dividing the observed ΔC_p (−1310 cal mol^{-1} K^{-1}) by this value, we estimate that 95 residues become solvent inaccessible upon complex formation. The enthalpy-based scaling factor is 0.70 kcal (mol res)$^{-1}$. Dividing the extrapolated $\Delta H(60)$ value for OCP1/OCP2 complex formation (−81.8 kcal mol^{-1}) by this value, we conclude that 117 residues are buried in the reaction. Although the exact number of residues that lose accessibility upon heterodimer formation is ambiguous and model-dependent, the conclusion that the association reaction is accompanied by a substantial degree of folding is unassailable.

Whether these disordered residues reside in OCP1 or OCP2, or both, is unknown. The ^{1}H,^{15}N HSQC spectrum of OCP2 (Fig. 5) suggests that the protein contains a disordered region. At the concentration employed for this experiment (2 mM), the protein will be completely dimeric. Although the spectrum exhibits reasonably good dispersion, a cluster of intense signals appears in the vicinity of 8.3 ppm, the proton chemical shift commonly associated with random coil amide signals. The intensity of the signals indicates that the associated amides enjoy a high degree of mobility. Potentially, some of these residues could become more ordered upon association with OCP1.

We do not have corresponding NMR data for OCP1. However, there is some evidence that the protein may contain one or more relatively unstructured regions. For example, the PEST domain (encompassing residues 1–54) is not visible in the electron density map of Skp1/Fbs1 [25], an indication that it is highly flexible. In addition, preliminary sedimentation velocity data on the protein (not shown) imply that the molecule is highly extended, which would be consistent with a loosely folded protein. Moreover, the binding of oligosaccharides by Fbs1 is strongly exothermic [41], suggesting that binding of the biological target provokes a significant conformational change in the C-terminal target-binding domain.

There is increasing awareness that many proteins harbor unstructured regions that become more ordered upon interaction with a suitable binding partner [42–44]. Proteins involved in signal transduction commonly exhibit this behavior because effective regulation requires that signaling complexes 1) associate rapidly and specifically following an appropriate stimulus and 2) dissociate promptly when signaling is complete. Coupled folding/binding events can produce highly specific, (relatively) low-affinity complexes capable of facile association/dissociation. Given the likelihood that OCP1 and OCP2 play a regulatory role in the cochlea, it is reasonable that they should exhibit this conformationally malleable signature.

5. Conclusions

The association of OCP1 with OCP2 exhibits a $\Delta G^{\circ\prime}$ of −10.4 kcal/mol. The reaction is enthalpically-driven (ΔH= −35.9 kcal/mol), entropically unfavorable ($-T\Delta S^{\circ\prime}$=25.5 kcal/mol), and is unaccompanied by protonation/deprotonation events. The enthalpy change is strongly temperature-dependent (ΔC_p= −1.31 kcal/mol). Analysis of the reaction entropy suggests that complex formation is associated with a substantial ordering of one or both polypeptide chains.

Acknowledgments

Through a contractual agreement with Washington University in St. Louis, this work was funded by NIH award NIDCD/NIH 01414 (to Dr. Isolde Thalmann, Department of Otolaryngology).

References

[1] S.S. Spicer, B.A. Schulte, Differences along the place-frequency map in the structure of supporting cells in the gerbil cochlea, Hear. Res. 79 (1994) 161–177.
[2] I. Thalmann, H.L. Rosenthal, B.W. Moore, R. Thalmann, Organ of Corti specific polypeptides: OCP-I and OCP-II, Otorhinolaryngology 226 (1980) 123–128.
[3] G.N. DeMartino, C.A. Slaughter, The proteasome, a novel protease regulated by multiple mechanisms, J. Biol. Chem. 274 (1999) 22123–22126.
[4] A.M. Weissman, Themes and variations on ubiquitylation, Nat. Rev., Mol. Cell Biol. 2 (2001) 169–178.
[5] C. Bai, P. Sen, K. Hofmann, L. Ma, M. Goebl, J.W. Harper, S.J. Elledge, SKP1 connects cell cycle regulators to the ubiquitin proteolysis machinery through a novel motif, the Fbox, Cell 86 (1996) 263–274.

[6] C. Connelly, P. Hieter, Budding yeast SKP1 encodes an evolutionaily conserved kinetochore protein required for cell cycle progression, Cell 86 (1996) 275–285.
[7] P.K. Jackson, A.G. Eldridge, E. Freed, L. Furstenthal, J.Y. Hsu, B.K. Kaiser, J.D.R. Reimann, The lore of the RINGs: substrate recognition and catalysis by ubiquitin ligases, Trends Cell Biol. 10 (2000) 429–439.
[8] S.A. Lyapina, C.C. Correll, E.T. Kipreos, R.J. Deshaies, Human CUL1 forms an evolutionarily conserved ubiquitin ligase complex (SCF) with SKP1 and an F-box protein, Proc. Natl. Acad. Sci. U. S. A. 95 (1998) 7451–7456.
[9] E.E. Patton, A.R. Willems, D. Sa, L. Kuras, D. Thomas, K.L. Craig, M. Tyers, Cdc53 is a scaffold protein for multiple Cdc34/Skp1/F-box protein complexes that regulate cell division and methionine biosynthesis in yeast, Genes Dev. 12 (1998) 692–705.
[10] Z.-K. Yu, J.L.M. Gervais, H. Zhang, Human CUL-1 associates with the SKP1/SKP2 complex and regulates $p21^{CIP1/WAF1}$ and cyclin D proteins, Proc. Natl. Acad. Sci. U. S. A. 95 (1998) 11324–11329.
[11] D. Skowyra, K.L. Craig, M. Tyers, S.J. Elledge, J.W. Harper, F-box proteins are receptors that recruit phosphorylated substrates to the SCF ubiquitin–ligase complex, Cell 91 (1997) 209–219.
[12] R.J. Deshaies, SCF and Cullin/Ring H2-based ubiquitin ligases, Annu. Rev. Cell Dev. Biol. 15 (1999) 435–467.
[13] Y. Liang, H. Chen, J.H. Asher, C.C. Chang, T.B. Friedman, Human inner ear OCP2 cDNA maps to 5q22–5q35.2 with related sequences on chromosomes 4p16.2–4p14, 5p13–5q22, 7pter–q22, 10 and 12p13–12qter, Gene 184 (1997) 163–167.
[14] M.T. Henzl, J. O'Neal, R. Killick, I. Thalmann, R. Thalmann, OCP1, an F-box protein, co-localizes with OCP2/SKP1 in the cochlear epithelial gap junction region, Hear. Res. 157 (2001) 100–111.
[15] J.A. Erhardt, W. Hynicka, A. DiBenedetto, N. Shen, N. Stone, H. Paulson, R.N. Pittman, A novel F box protein, NFB42, is highly enriched in neurons and induces growth arrest, J. Biol. Chem. 273 (1998) 35222–35227.
[16] M.T. Henzl, I. Thalmann, J.D. Larson, E.G. Ignatova, R. Thalmann, The cochlear F-box protein OCP1 associates with OCP2 and connexin 26, Hear. Res. 191 (2004) 101–109.
[17] F. Delaglio, S. Grzesiek, G.W. Vuister, G. Zhu, J. Pfeifer, A. Bax, NMRPipe: a multidimensional spectral processing system based on UNIX pipes, J. Biomol. NMR 6 (1995) 277–293.
[18] T.D. Goddard, D.G. Kneller, Sparky 3, , 2007.
[19] A.T. Brunger, P.D. Adams, G.M. Clore, W.L. DeLano, P. Gros, R.W. Grosse-Kunstleve, J.S. Jiang, J. Kuszewski, M. Nilges, N.S. Pannu, R.J. Read, L.M. Rice, T. Simonson, G.L. Warren, Crystallography & NMR system: a new software suite for macromolecular structure determination, Acta Crystallogr., D 54 (1998) 905–921.
[20] H. Fukada, K. Takahashi, Enthalpy and heat capacity changes for the proton dissociation of various buffer components in 0.1 M potassium chloride, Proteins 33 (1998) 159–166.
[21] R.N. Goldberg, N. Kishore, R.M. Lennen, Thermodynamic quantities for the ionization reactions of buffers, J. Phys. Chem. Ref. Data 31 (2002) 231–370.
[22] Y. Yoshida, T. Chiba, F. Tokunaga, H. Kawasaki, K. Iwai, T. Suzuki, Y. Ito, K. Matsuoka, M. Yoshida, K. Tanaka, E3 ubiquitin ligase that recognizes sugar chains, Nature 418 (2002) 438–442.
[23] R. Thalmann, M.T. Henzl, R. Killick, E.G. Ignatova, I. Thalmann, Toward an understanding of cochlear homeostasis: the impact of location and the role of OCP1 and OCP2, Acta Oto-laryngol. 123 (2003) 203–208.
[24] H. Schulman, A.C. Carrano, P.D. Jeffrey, Z. Bowen, E.R.E. Kinnucan, M.S. Finnin, S.J. Elledge, J.W. Harper, M. Pagano, N.P. Pavletich, Insights into SCF ubiquitin ligases from the structure of the Skp1–Skp2 complex, Nature 408 (2000) 381–386.
[25] T. Mizushima, Y. Yoshida, T. Kumanomidou, Y. Hasegawa, A. Suzuki, T. Yamane, K. Tanaka, Structural basis for the selection of glycosylated substrates by SCF^{FBs1} ubiquitin ligase, Proc. Natl. Acad. Sci. U. S. A. 104 (2007) 5777–5781.
[26] M.T. Henzl, I. Thalmann, R. Thalmann, OCP2 exists as a dimer in the organ of Corti, Hear. Res. 126 (1998) 37–46.
[27] B.M. Baker, K.P. Murphy, Dissecting the energetics of a protein–protein interaction: the binding of ovomucoid third domain to elastase, J. Mol. Biol. 268 (1997) 557–569.
[28] D.G. Myszka, R.W. Sweet, P. Hensley, M. Brigham-Burke, P.D. Kwong, W.A. Hendrickson, R. Wyatt, J. Sodroski, M.L. Doyle, Energetics of the HIV gp120-CD4 binding reaction, Proc. Natl. Acad. Sci. U. S. A. 97 (2000) 9026–9031.
[29] D. Xie, E. Freire, Structure based prediction of protein folding intermediates, J. Mol. Biol. 242 (1994) 62–80.
[30] K.P. Murphy, E. Freire, Thermodynamics of structural stability and cooperative folding behavior in proteins, Adv. Protein Chem. 43 (1992) 313–361.
[31] A.D. Robertson, K.P. Murphy, Protein structure and the energetics of protein stability, Chem. Rev. 97 (1997) 1251–1267.
[32] R.L. Baldwin, Temperature dependence of the hydrophobic interaction in protein folding, Proc. Natl. Acad. Sci. U. S. A. 83 (1986) 8069–8072.
[33] K.P. Murphy, P.L. Privalov, S.J. Gill, Common features of protein unfolding and dissolution of hydrophobic compounds, Science 247 (1990) 559–561.
[34] A.V. Finkelstein, J. Janin, The price of lost freedom; entropy of bimolecular complex formation, Protein Eng. 3 (1989) 1–3.
[35] B. Tidor, M. Karplus, The contribution of vibrational entropy to molecular association. The dimerization of insulin, J. Mol. Biol. 238 (1994) 414.
[36] J. Janin, C. Chothia, The structure of protein–protein recognition sites, J. Biol. Chem. 265 (1990) 16027–16030.
[37] M.S. Searle, D.H. Williams, The cost of conformational order: entropy changes in molecular associations, J. Am. Chem. Soc. 114 (1992) 10690–10697.
[38] R.S. Spolar, J. Record, Coupling of local folding to site-specific binding of proteins to DNA, Science 263 (1994) 777–784.
[39] L.M. Amzel, Loss of translational entropy in binding, folding and catalysis, Proteins 29 (1997) 1–6.
[40] A. Tamura, P.L. Privalov, The entropy cost of protein association, J. Mol. Biol. 273 (1997) 1048–1060.
[41] S. Hagihara, K. Totani, I. Matsuo, Y. Ito, Thermodynamic analysis of interactions between N-linked sugar chains and F-box protein Fbs1, J. Med. Chem. 48 (2005) 3126–3129.
[42] H.J. Dyson, P.E. Wright, Coupling of folding and binding for unstructured proteins, Curr. Opin. Struck. Biol. 12 (2002) 54–60.
[43] P. Tompa, Intrinsically unstructured proteins, Trends Biochem. Sci. 27 (2002) 527–533.
[44] H.J. Dyson, P.E. Wright, Intrinsically unstructured proteins and their functions, Nat. Rev., Mol. Cell Biol. 6 (2005) 197–208.
[45] W.L. DeLano, The PyMOL Molecular Graphics System, , 2002.